34 J. Phys. Chem. A 2000, 104, 34−44

Calculated Vibrational Spectra for CH_nOH_m Species

Paul Blowers and Richard I. Masel*

Department of Chemical Engineering, University of Illinois at Urbana−Champaign, 600 S. Mathews Avenue, Urbana, Illinois 61801-3792

Received: July 12, 1999; In Final Form: October 6, 1999

There is a lack of reference vibrational spectra in the literature for many species that have been postulated to form on metal surfaces. In this paper we calculate high-quality reference spectra for a series of molecules of the form CH_nOH_m. Specifically, we looked at the neutral, charged, and excited charged forms of CH_3OH, CH_3O, CH_3OH_2, CH_2O, CH_2OH, CHO, and HCOH. These calculations were done using scaled MP2(full)/6-31g*, scaled B3LYP/6-31g*, scaled QCIST/6-31g*, and scaled MP2/6-311+G(2d,p) level. The result is a consistent set of reference spectra for a series of molecules of current interest.

Introduction

Surface scientists often must differentiate among many similar species as they look at what is forming on a particular surface.[1−3] Despite the long history of surface experiments, good vibrational reference spectra are often lacking for common molecules and possible species. In these cases, gas-phase infrared spectra are used when reference spectra are not readily available for the species of interest. In many cases, too, available spectra are incomplete and several peaks may be lacking. Oxygenates on surfaces cause particular problems because many different species can form and there are no suitable reference spectra for many of these species.[4−14]

In this work, we calculated the vibrational spectra for the neutral, charged, and excited charged states of CH_3OH, CH_3O, CH_3OH_2, CH_2O, CH_2OH, CHO, and HCOH. The species are candidates for possible intermediates during methanol adsorption on Pt(110). Although calculations have been done for some of these species,[15−27] consistent reference spectra of the same level of calculation or from experiments are not available for many of these species. There is reason to suspect that some of the species can form on surfaces. The objective of this paper is to calculate reference spectra that we can then compare to data to identify surface species.

In the work here we used ab initio methods to compute frequencies for the CH_nOH_m species that have been postulated to form on metal surfaces. We also did triplet (i.e., radical) states of some of the species, since triplet states can be stabilized on transition metal surfaces (e.g., di-σ-ethylene is a triplet state).

Procedures

The calculations were done with the Gaussian 92 or Gaussian 98 program.[28−29] Generally, we followed the method of Pople et al.,[30−31] Scott and Radom,[32] and Wong[33] to calculate the reference spectra.

Vibrational frequencies were calculated using three different computational procedures: scaled MP2, scaled B3LYP, and scaled QCISD calculations where the scaling factors come from the work of Pople et al.,[30,31] Scott and Radom,[32] and Wong.[33] Scaled MP2 is the most popular procedure used to estimate vibrational frequencies in the current literature. It is the default for the ZPE correction in G-2 and G-3 calculations. Pople et al. and Radom et al. examined the accuracy of the method and found that for a variety of species the average error is 67 cm^{-1}, i.e., less than the typical shift in an HREELS peak with coverage.

B3LYP has also been used extensively in the literature. Wong found that it often gave better vibrational frequencies than MP2. However, oxygenates are an exception where MP2 is better. Wong did not test B3LYP for triplet states. However, M. Head-Gordon[45] showed that B3LYP and other density functional methods have a special problem for excited states.

QCISD frequencies are also being reported here. QCISD gives much better bond energies than MP2, but in the current literature, QCISD is rarely used to calculate vibrational frequencies. Recall that vibrational frequencies are calculated from the second derivative of the energy with respect to atomic displacements. In MP2 and B3LYP methods the second derivatives can be calculated analytically. However, with QCISD, the derivatives must be calculated by perturbing the system in all directions and numerically differentiating the forces. The numerical differentiation introduces error when the potential is asymmetric.

One of the reviewers had suggested that we also calculate vibrational frequencies via CCSD. However, CCSD frequencies are not supported in Gaussian 98 and it requires that one calculate a second derivative numerically, which often leads to significant error.

Finally, it should be noted that most of the calculations were done with a 6-31G* basis set. This would be considered a small basis for ab initio calculations. However, this is the basis set that is used most often in vibrational calculations. Some years ago, Pople et al.,[30−31] Radom et al.,[32] and Wong et al.[33] showed that scaled 6-31G* calculations give quite reasonable vibrational frequencies, and they published the scale factors. QCISD scale factors are not available for any other basis set. We have also calculated frequencies at the MP2/6-311+g(2d,p) level to check our results. However, MP2/6-311+g(2d,p) frequencies are not often reported in the literature, so their accuracy is unknown.

All the calculations were done for the gas phase. We did selective calculations with a single metal atom present and did not observe significant peak shifts. However, we do not know whether there would be shifts if more metal atoms were used.

---

* To whom correspondence should be addressed.

10.1021/jp992343t CCC: $19.00

TABLE 1: Comparison of the Properties Calculated for Methanol to Those from Experiment[a]

	method					
	MP2(full)/6-31G*	B3LYP/6-31G*	QCISD/6-31G*	MP2/6-311+G(2d,p)	MP2/6-311+G(2d,p)	expt[35,38]
trans, $R_{\mathrm{H-C}}$, Å	1.097	1.101	1.100	1.0936	1.0936	1.094
cis, $R_{\mathrm{H-C}}$, Å	1.089	1.094	1.094	1.0877	1.0877	1.094
$R_{\mathrm{O-C}}$, Å	1.423	1.419	1.425	1.425	1.425	1.417
$R_{\mathrm{O-H}}$, Å	0.970	0.968	0.970	0.963	0.963	0.981
A_{HCO} (deg)	112.3	112.7	112.2	111.9	111.9	110
A_{HCO} (deg)	106.3	106.6	106.4	106.5	106.5	110
A_{COH} (deg)	107.4	107.6	107.5	108.0	108.0	108
frequency scaling factor	0.9427	0.9614	0.9537	unscaled	0.96	
torsion, cm^{-1}	298	331	319	293	281	272
CO stretch, cm^{-1}	1022	1024	1034	1053	1011	1034
CH_3 s-rock, cm^{-1}	1051	1054	1057	1093	1049	1077
CH_3 a-rock, cm^{-1}	1136	1138	1141	1196	1148	1145
OH bend, cm^{-1}	1337	1346	1357	1382	1327	1334
CH_3 s-deform., cm^{-1}	1452	1453	1456	1512	1452	1452
CH_3 a-deform., cm^{-1}	1476	1466	1475	1535	1473	1466
CH_3 a-deform., cm^{-1}	1489	1482	1488	1547	1485	1473
CH_3 stretch, cm^{-1}	2901	2880	2891	3054	2932	2848
CH_3 stretch, cm^{-1}	2964	2921	2944	3122	2997	2962
CH_3 stretch, cm^{-1}	3039	3010	3017	3184	3056	3006
CH_3 stretch, cm^{-1}	3579	3611	3601	3868	3714	3667
rms error, cm^{-1}	19.9	21.2	21.1	72	26.9	

[a] The vibrations are designated by their conventional designations (all are really combination modes).

TABLE 2: Comparison of the Properties Calculated for Methoxy to Those from Experiment[a]

	method						
	MP2(full)/6-31G*	B3LYP/6-31G*	QCISD/6-31G* (minimum energy structure)	QCISD/6-31G* (C_s structure)	MP2/6-311 +G(2d,p)	MP2/6-311 +G(2d,p)	expt[34,37]
$\langle s^2 \rangle$ before spin projection	0.7577	0.7529	NA	NA	0.7593	0.7593	0.75
$R_{\mathrm{H-C}}$, Å	1.096	1.103	1.106	1.106	1.100	1.100	1.100
$R_{\mathrm{H-C}}$, Å	1.101	1.110	1.100	1.100	1.094	1.094	1.100
$R_{\mathrm{O-C}}$, Å	1.387	1.366	1.389	1.389	1.381	1.381	1.370
A_{OCH} (deg)	104.8	105.3	105.1	105.1	104.9	104.9	109
A_{OCH} (deg)	112.4	113.5	112.5	112.5	112.3	112.3	109
frequency scaling factor	0.9427	0.9496	0.9537	0.9537	1.00	0.96	NA
ν_1, cm^{-1}	794	898	−7572	482	802	770	653
ν_2, cm^{-1}	943	942	−4621	972	975	936	NR
ν_3, cm^{-1}	1077	1084	673	978	1116	1071	1047
ν_4, cm^{-1}	1382	1346	1144	1382	1433	1375	1362
ν_5, cm^{-1}	1399	1354	1317	1082	1442	1385	NR
ν_6, cm^{-1}	1492	1489	1875	1494	1551	1489	1497
ν_7, cm^{-1}	2871	2805	2871	2849	3009	2889	?
ν_8, cm^{-1}	2952	2871	5438	2875	3091	2967	2840
ν_9, cm^{-1}	2982	2907	8165	2921	3129	3004	?
rms error, cm^{-1}	66.6	112.1	3660	83.1	113.7	58.0	

[a] NR = not resolved. Note the lowest energy state has C_1 symmetry at the QCISD/6-31G* level and C_s symmetry in all the other calculations. The vibrational frequencies calculated for the C_1 state had numerical difficulties, so the reviewer insisted that we provide C_s frequencies as well. The C_s vibrational frequencies are not considered meaningful (see text).

TABLE 3: Comparison of the Formaldehyde (H_2CO) Results to Those from Experiment[a]

	method					
	MP2(full)/6-31G*	B3LYP/6-31G*	QCISD/6-31G*	MP2/6-311+g(2d,p)	MP2/6-311+ g(2d,p)	expt[35,38]
R_{CO}	1.220	1.206	1.217	1.213	1.213	1.203
R_{CH} (deg)	1.104	1.110	1.107	1.103	1.103	1.099
A_{HH} (deg)	122.2	122.3	122.14	121.7	121.7	121.8
frequency scaling factor	0.9427	0.9614	0.9537	unscaled	0.96	
CH_2 wag, cm^{-1}	1144	1151	1145	1185	1138	1167
CH_2 rock, cm^{-1}	1222	1230	1232	1280	1229	1249
CH_2 scissors, cm^{-1}	1494	1502	1501	1550	1488	1500
CO stretch, cm^{-1}	1689	1778	1734	1747	1678	1746
CH_2 s-stretch, cm^{-1}	2840	2806	2837	2963	2844	2932
CH_2 a-stretch, cm^{-1}	2907	2856	2898	3039	2918	2953
rms error, cm^{-1}	50.2	67	46.5	45	50	

[a] The vibrations are designated by their conventional designations (all are really combination modes).

Results of Calculations

Tables 1−20 give the results of the calculations. Table 1 compares the geometries and vibrational frequencies calculated for methanol to those reported in the literature. Generally, the geometries agree at all levels of calculations and agree quite well with those determined from experiments. The average error

TABLE 4: Comparison of the Calculated Properties of Formyl Radicals, [HCO]

	method					
	MP2(full)/6-31G*	B3LYP/6-31G*	QCISD/6-31G*	MP2/6-311+G(2d,p)	MP2/6-311+G(2d,p)	expt[41−43]
$\langle s^2 \rangle$ before spin projection	0.7653	0.7524	NA	0.7658	0.7658	0.75
R_{H-C}, Å	1.123	1.129	1.125	1.121	1.121	1.119
R_{O-C}, Å	1.191	1.183	1.192	1.183	1.183	1.175
A_{CH} (deg)	123.4	123.6	124.3	123.8	123.8	124.4
frequency scaling factor	0.9427	0.9614	0.9537	unscaled	0.96	
ν_1, cm^{-1}	1071	1088	1106	1131	1086	1087
ν_2, cm^{-1}	1905	1873	1803	1909	1832	1868
ν_3, cm^{-1}	2591	2557	2589	2739	2629	2435
rms error, cm^{-1}	92.75	70.61	97.58	179.44	113.95	

TABLE 5: Calculated Properties of the Ground State of Formyl Ions, $[HCO]^+$

	method				
	MP2(full)/ 6-31G*	B3LYP/ 6-31G*	QCISD/ 6-31G*	MP2/6-311 +G(2d,p)	MP2/6-311 +G(2d,p)
R_{H-C}, Å	1.095	1.099	1.097	1.093	1.093
R_{O-C}, Å	1.131	1.113	1.122	1.181	1.181
A_{CH} (deg)	180.	180.	180.	180.	180.
frequency scaling factor	0.9427	0.9614	0.9537	unscaled	0.96
ν_1, cm^{-1}	806	834	811	846	812
ν_2, cm^{-1}	2015	2179	2112	2128	2043
ν_3, cm^{-1}	3114	3134	3138	3238	3109

TABLE 6: Calculated Properties of the Triplet ($^3A_1$) State of Formyl Ions, $[HCO]^+$

	method				
	MP2/ 6-31G*	B3LYP/ 6-31G*	QCISD/ 6-31G*	MP2/6-311 +G(2d,p)	MP2/6-311 +G(2d,p)
$\langle s^2 \rangle$ before spin projection	2.0072	2.0024	NA	2.0090	2.0090
R_{H-C}, Å	1.102	1.1147	1.109	1.104	1.104
R_{O-C}, Å	1.277	1.2741	1.282	1.269	1.269
A_{CH} (deg)	119.2	117.6	117.6	118.9	118.9
frequency scaling factor	0.9427	0.9614	0.9537	unscaled	0.96
ν_1, cm^{-1}	984	937	957	1031	990
ν_2, cm^{-1}	1526	1507	1480	1597	1553
ν_3, cm^{-1}	2940	2828	2893	3048	2926

TABLE 7: Calculated Properties of the Ground ($^2B_2$) State of Formaldehyde Cations, $[H_2CO]^+$

	method				
	MP2(full)/ 6-31G*	B3LYP/ 6-31G*	QCISD/ 6-31G*	MP2/6-311 +g(2d,p)	MP2/6-311 +g (2d,p)
$\langle s^2 \rangle$ before spin projection	0.786	0.758	NA	0.786	0.786
R_{H-C}, Å	1.108	1.118	1.113	1.111	1.111
R_{O-C}, Å	1.207	1.200	1.214	1.195	1.195
A_{OCH} (deg)	118.4	119.8	119.1	118.4	118.4
frequency scaling factor	0.9427	0.9614	0.9537	unscaled	0.96
ν_1, cm^{-1}	853	836	862	875	840
ν_2, cm^{-1}	1067	1030	1039	1106	1062
ν_3, cm^{-1}	1264	1225	1247	1316	1263
ν_4, cm^{-1}	1551	1638	1582	1627	1562
ν_5, cm^{-1}	2778	2723	2769	2862	2747
ν_6, cm^{-1}	2919	2811	2879	3009	2889

TABLE 8: Calculated Properties of the $^4A''$ (Excited) State of Formaldehyde Cations, $[H_2CO]^{+\,a}$

	method				
	MP2(full)/ 6-31G*	B3LYP/ 6-31G*	QCISD/ 6-31G*	MP2/6-311 +g(2d,p)	MP2/6-311 +g (2d,p)
$\langle s^2 \rangle$ before spin projection	3.768	3.755	NA	3.770	3.770
R_{H-C}, Å	1.090	1.114	1.098	1.089	1.089
R_{O-C}, Å	1.527	1.448	1.521	1.520	1.520
A_{OCH} (deg)	107.0	108.52	107.4	106.9	106.9
frequency scaling factor	0.9427	0.9614	0.9537	unscaled	0.96
ν_1, cm^{-1}	621	669	612	659	632
ν_2, cm^{-1}	829	786	818	874	839
ν_3, cm^{-1}	900	911	868	934	897
ν_4, cm^{-1}	1292	1164	1252	1355	1301
ν_5, cm^{-1}	2960	2761	2914	3085	2962
ν_6, cm^{-1}	3127	2834	3069	3259	3129

[a] Note this state is nonplanar.

TABLE 9: Calculated Properties of the Ground State of *cis*-Hydroxymethylene Diradicals, [HCOH]

	method				
	MP2(full)/ 6-31G*	B3LYP/ 6-31G*	QCISD/ 6-31G*	MP2/6-311 +G(2d,p)	MP2/6-311 +G(2d,p)
R_{H-C}, Å	1.121	1.129	1.129	1.116	1.116
R_{O-C}, Å	1.316	1.312	1.323	1.312	1.312
R_{O-H}, Å	0.983	0.986	0.983	0.975	0.975
A_{HCO} (deg)	106.56	106.7	106.3	106.9	106.9
A_{COH} (deg)	115.6	116.8	115.4	114.4	114.4
frequency scaling factor	0.9427	0.9614	0.9537	unscaled	0.96
ν_1, cm^{-1}	999	979	968	1045	1003
ν_2, cm^{-1}	1198	1185	1208	1237	1188
ν_3, cm^{-1}	1298	1293	1276	1340	1286
ν_4, cm^{-1}	1425	1434	1432	1496	1436
ν_5, cm^{-1}	2687	2621	2627	2859	2745
ν_6, cm^{-1}	3350	3282	3375	3641	3495

TABLE 10: Calculated Properties of the Ground State of *cis*-Hydroxymethylene Radical Cations, $[HCOH]^+$

	method				
	MP2(full)/ 6-31G*	B3LYP/ 6-31G*	QCISD/ 6-31G*	MP2/6-311 +G(2d,p)	MP2/6-311 +G(2d,p)
$\langle s^2 \rangle$ before spin projection	0.7623	0.7531	NA	0.7620	0.7620
R_{H-C}, Å	1.099	1.105	1.102	1.100	1.100
R_{O-C}, Å	1.224	1.218	1.227	1.216	1.216
R_{O-H}, Å	1.004	1.002	1.002	0.995	0.995
A_{HCO} (deg)	131.8	131.8	131.5	131.4	131.4
A_{COH} (deg)	120.6	122.2	120.8	119.7	119.7
frequency scaling factor	0.9427	0.9614	0.9537	unscaled	0.96
ν_1, cm^{-1}	894	869	889	937	900
ν_2, cm^{-1}	933	933	953	991	952
ν_3, cm^{-1}	1116	1086	1119	1192	1144
ν_4, cm^{-1}	1661	1682	1647	1738	1668
ν_5, cm^{-1}	2977	2936	2971	3089	2966
ν_6, cm^{-1}	3174	3176	3219	3442	3304

in the bond length is only 0.02 Å, while the average error for angles is only 0.59°. The MP2/6-31G*, B3LYP/6-31G*, and QCISD/6-31G* frequencies are all very similar and show good agreement with experimental results. The rms error is slightly smaller with MP2/6-31G* than with the other methods. This is consistent with the previous results of Pople et al. and Radom et al. who also found that MP2/6-31G* is unexpectedly good for oxygenates.

We also include MP2/6-311+G(2d,p) frequencies in Table 1. Generally, the unscaled MP2/6-311+G(2d,p) frequencies only show poor agreement with those from experiment. We find that if we scale the MP2/6-311+G(2d,p) frequencies by an arbitrary factor of 0.96, chosen to minimize the rms error in the calculations, we get reasonable agreement with experimental results. Still, the agreement is not as good as with MP2/6-31G*.

In the tables that follow we will include both the scaled and

TABLE 11: Calculated Properties of the Ground State of *trans*-Hydroxymethylene Diradicals, [HCOH]

	method				
	MP2(full)/ 6-31G*	B3LYP/ 6-31G*	QCISD/ 6-31G*	MP2/6-311 +G(2d,p)	MP2/6-311 +G(2d,p)
$R_{\mathrm{H-C}}$, Å	1.113	1.122	1.121	1.108	1.108
$R_{\mathrm{O-C}}$, Å	1.322	1.321	1.328	1.313	1.313
$R_{\mathrm{O-H}}$, Å	0.975	0.976	0.977	0.970	0.970
A_{HCO} (deg)	101.5	101.2	101.3	102.3	102.3
A_{COH} (deg)	107.3	108.0	107.5	107.8	107.8
frequency scaling factor	0.9427	0.9614	0.9537	unscaled	0.96
ν_1, cm^{-1}	1075	1056	1048	1124	1079
ν_2, cm^{-1}	1164	1176	1178	1220	1171
ν_3, cm^{-1}	1290	1278	1268	1336	1283
ν_4, cm^{-1}	1461	1476	1471	1521	1461
ν_5, cm^{-1}	2787	2717	2727	2952	2834
ν_6, cm^{-1}	3474	3495	3503	3729	3579

TABLE 12: Calculated Properties of the Ground State of *trans*-Hydroxymethylene Radical Cations, $[HCOH]^+$

	method				
	MP2(full)/ 6-31G*	B3LYP/ 6-31G*	QCISD/ 6-31G*	MP2/6-311 +G(2d,p)	MP2/6-311 +G(2d,p)
$\langle s^2 \rangle$ before spin projection	0.7596	0.7524	NA	0.7603	0.7603
$R_{\mathrm{H-C}}$, Å	1.096	1.104	1.100	1.098	1.098
$R_{\mathrm{O-C}}$, Å	1.230	1.225	1.234	1.222	1.222
$R_{\mathrm{O-H}}$, Å	1.002	0.998	0.999	0.993	0.993
A_{CH} (deg)	123.9	123.9	123.7	124.4	124.4
A_{OH} (deg)	117.7	119.0	117.8	117.1	117.1
frequency scaling factor	0.9427	0.9614	0.9537	unscaled	0.96
ν_1, cm^{-1}	928	900	921	968	930
ν_2, cm^{-1}	950	944	962	1012	972
ν_3, cm^{-1}	1196	1192	1215	1262	1211
ν_4, cm^{-1}	1636	1654	1619	1171	1124
ν_5, cm^{-1}	2999	2958	2995	3108	2984
ν_6, cm^{-1}	3227	3279	3293	3487	3347

TABLE 13: Calculated Properties of the Ground State of Hydroxymethyl Radicals, $[H_2COH]$

	method				
	MP2(full)/ 6-31G*	B3LYP/ 6-31G*	QCISD/ 6-31G*	MP2/6-311 +g(2d,p)	MP2/6-311 +g(2d,p)
$\langle s^2 \rangle$ before spin projection	0.759	0.753	NA	0.7613	0.7613
$R_{\mathrm{O-C}}$, Å	1.373	1.370	1.377	1.369	1.369
$R_{\mathrm{H-C}}$, Å	1.082	1.089	1.090	1.082	1.082
$R_{\mathrm{O-H}}$, Å	0.971	0.969	0.971	0.963	0.963
A_{OCH} (deg)	118.2	118.5	118.15	118.3	118.3
A_{OCH} (deg)	112.2	112.6	112.3	113.0	113.0
frequency scaling factor	0.9427	0.9614	0.9537	unscaled	0.96
ν_1, cm^{-1}	435	434	427	441	423
ν_2, cm^{-1}	736	655	715	682	655
ν_3, cm^{-1}	1035	1031	1038	1079	1036
ν_4, cm^{-1}	1161	1172	1159	1199	1151
ν_5, cm^{-1}	1323	1328	1340	1380	1325
ν_6, cm^{-1}	1459	1444	1454	1525	1464
ν_7, cm^{-1}	3019	3005	3004	3179	3052
ν_8, cm^{-1}	3164	3144	3139	3330	3197
ν_9, cm^{-1}	3581	3613	3603	3861	3706

unscaled MP2/6-311+G(2d,p) frequencies, since the 0.96 scaling factor is not justified except by the fact that we get better agreement with experimental results when we include it.

Table 2 compares our calculated frequencies to the experimentally determined ones for methoxy (CH_3O). In this case all the methods predict geometries that agree well with those from experiment but only MP2 predicts frequencies that show reasonable agreement with experimental results.

TABLE 14: Calculated Properties of the Ground State of Hydroxymethyl Cations, $[H_2COH]^+$

	method				
	MP2(full)/ 6-31G*	B3LYP/ 6-31G*	QCISD/ 6-31G*	MP2/6-311 +g(2d,p)	MP2/6-311 +g(2d,p)
$R_{\mathrm{O-C}}$, Å	1.256	1.252	1.259	1.369	1.369
$R_{\mathrm{H-C}}$, Å	1.088	1.092	1.090	1.082	1.082
$R_{\mathrm{H-C}}$, Å	1.088	1.094	1.090	1.078	1.078
$R_{\mathrm{O-H}}$, Å	0.994	0.989	0.992	0.963	0.963
A_{OCH}	115.3	122.02	115.4	118.3	118.3
A_{OCH} (deg)	115.3	115.55	115.3	113.0	113.0
frequency scaling factor	0.9427	0.9614	0.9537	unscaled	0.96
ν_1, cm^{-1}	1006	987	994	1052	1010
ν_2, cm^{-1}	1067	1072	1079	1129	1084
ν_3, cm^{-1}	1193	1190	1188	1250	1200
ν_4, cm^{-1}	1321	1328	1341	1402	1346
ν_5, cm^{-1}	1433	1430	1424	1507	1447
ν_6, cm^{-1}	1605	1616	1596	1681	1614
ν_7, cm^{-1}	3014	3004	3014	3133	3007
ν_8, cm^{-1}	3161	3142	3155	3286	3155
ν_9, cm^{-1}	3327	3398	3386	3594	3450

TABLE 15: Calculated Properties of the Triplet (^3A) State of Hydroxymethyl Cations, $[H_2COH]^+$

	method				
	MP2(full)/ 6-31G*	B3LYP/ 6-31G*	QCISD/ 6-31G*	MP2/6-311 +g(2d,p)	MP2/6-311 +g(2d,p)
$\langle s^2 \rangle$ before spin projection	2.011	2.004	NA	2.024	2.024
$R_{\mathrm{O-C}}$, Å	1.354	1.327	1.364	1.265	1.265
$R_{\mathrm{H-C}}$, Å	1.106	1.126	1.112	1.172	1.172
$R_{\mathrm{O-H}}$, Å	1.005	1.000	1.006	0.984	0.984
A_{OCH} (deg)	110.3	112.7	111.0	117.1	117.1
A_{OCH} (deg)	114.5	112.7	114.2	117.1	117.1
A_{OCH} (deg)	115.3	115.55	115.3	115.7	115.7
frequency scaling factor	0.9427	0.9614	0.9537	unscaled	0.96
ν_1, cm^{-1}	574	623	629	564	542
ν_2, cm^{-1}	605	733	717	876	841
ν_3, cm^{-1}	913	962	965	901	865
ν_4, cm^{-1}	992	1033	971	1128	1083
ν_5, cm^{-1}	1064	1083	1070	1221	1172
ν_6, cm^{-1}	1234	1217	1215	1880	1805
ν_7, cm^{-1}	2767	2660	2771	2114	2030
ν_8, cm^{-1}	2891	2665	2853	2899	2783
ν_9, cm^{-1}	3211	3264	3238	3615	3470

TABLE 16: Calculated Properties of the Triplet (^3A) State of Methoxy Cations, $[H_3CO]^+$ [a]

	method				
	MP2(full)/ 6-31G*	B3LYP/ 6-31G*	QCISD/ 6-31G*	MP2/6-311 +G(2d,p)	MP2/6-311 +G(2d,p)
$\langle s^2 \rangle$ before spin projection	2.027	2.028	NA	2.0032	2.0032
$R_{\mathrm{O-C}}$, Å	1.310	1.306	1.335	1.299	1.299
$R_{\mathrm{H-C}}$, Å	1.119	1.129	1.120	1.120	1.120
A_{OCH} (deg)	108.2	109.5	108.3	108.5	108.5
frequency scaling factor	0.9427	0.9614	0.9537	unscaled	0.96
ν_1, cm^{-1}	818	846	865	837	803
ν_2, cm^{-1}	818	846	865	837	803
ν_3, cm^{-1}	1056	1126	1059	1113	1068
ν_4, cm^{-1}	1158	1126	1195	1184	1137
ν_5, cm^{-1}	1159	1187	1195	1184	1137
ν_6, cm^{-1}	1247	1227	1255	1287	1236
ν_7, cm^{-1}	2653	2632	2695	2761	2651
ν_8, cm^{-1}	2723	2652	2761	2862	2748
ν_9, cm^{-1}	2725	2653	2761	2827	2714

[a] Note that we have not found a stable singlet. Instead the singlet structure isomerizes to a hydroxymethyl cation. The triplet state is stable. The triplet state almost has C_{3v} symmetry, but the electronic structure is not well defined in C_{3v}.

We believe that the poor agreement of B3LYP/6-31G* is associated with the instability of the methoxy radicals. Recall that methoxy radicals are barely stable. One can observe them spectroscopically, but they readily isomerize to hydroxymethyl (CH_2OH) radicals. In our work we found that B3LYP did not

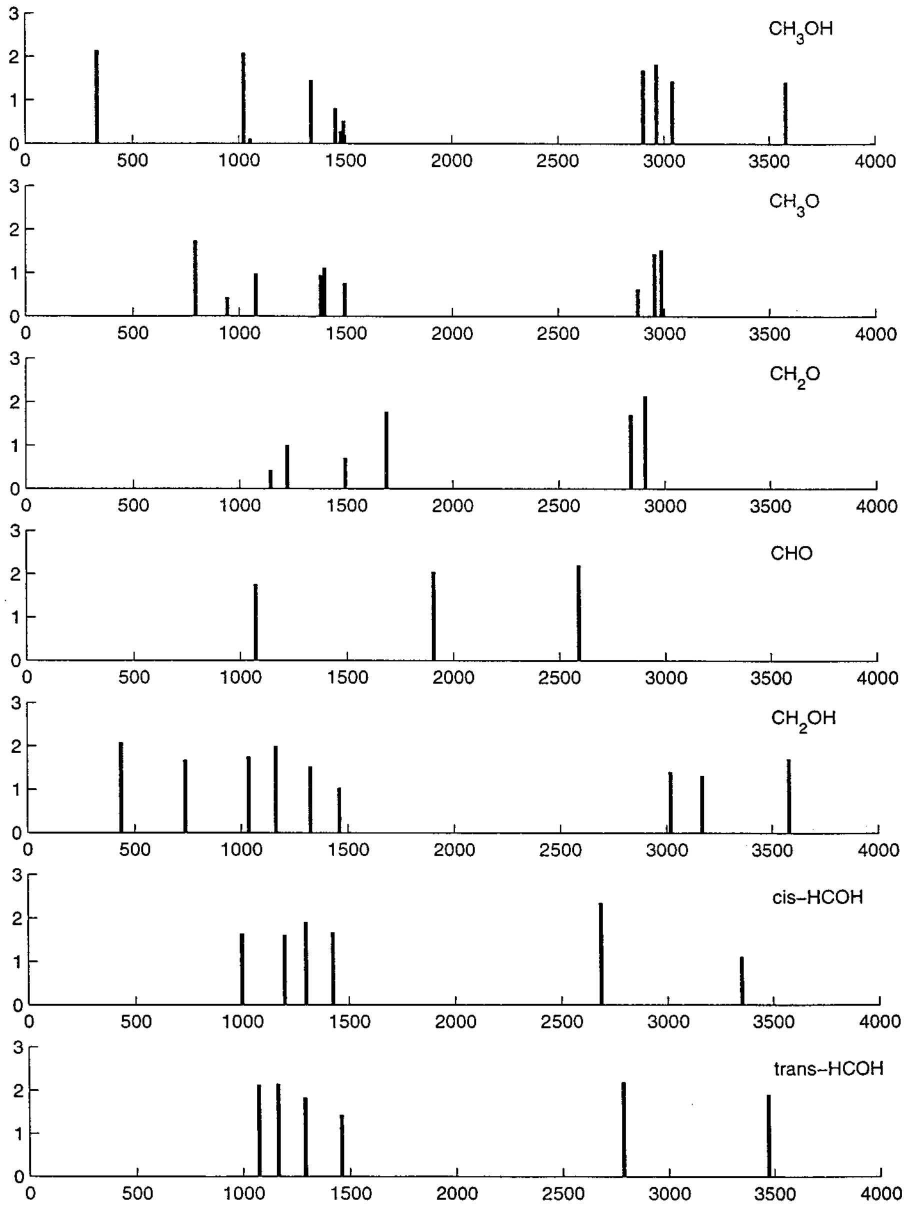

Figure 1. Neutral species reference spectra calculated at the MP2(full)/6-31g* level. Plots are log(calculated intensity in arbitrary units) vs wavenumber (cm^{-1}).

give good vibrational frequencies for methoxy presumably because the methoxy is, in a sense, an excited state of the system.

QCISD had some numerical instabilities for methoxy. The lowest energy structure of methoxy had C_s symmetry in the MP2 and B3LYP calculations. However, a structure with C_1 symmetry has slightly lower energy than the C_s structure at the QCISD/6-31G* level. Unfortunately, Gaussian had numerical difficulties calculating the vibrational frequencies of the C_1 structure. (The numerical differentiation caused instabilities.) One does get reasonable frequencies if one forces the molecule into a C_s structure. The C_s structure is not a stationary point, so it is unclear that the C_s results are meaningful. However, we include them as well.

Table 3 shows results for formaldehyde. The vibrational frequencies agree with the experimental results to within the accuracy of a typical EELS experiment, and the bond lengths are accurate with an average error of 0.02 Å.

Tables 4−6 show the geometries and vibrational frequencies of several formyl (HCO) species. Generally, the geometries were consistent at all levels of calculation. The vibrational frequencies are also similar at all levels of calculation except that the triplet state of formyl radicals has some numerical difficulties at the QCISD/6-31G* level. None of the calculations show wonderful agreement with vibrational data from fluorescence experiments.[41−42] This is associated with a special problem with calculating vibrational frequencies of formyl radicals discussed by Serrano-Andres et al.[44] Serrano-Andres et al. show that one can obtain more accurate vibrational frequencies for HCO by including the asymmetric correction in the vibrational calculation. The asymmetric correction would change near a surface, so we decided to not consider them in the work here.

Tables 7−12 show the calculated geometries and vibrational frequencies for a number of H_2CO and HCOH species. In all cases the molecules are stable. There are some small differences among the vibrational frequencies at the various levels of calculation. However, all the frequencies are the same within the uncertainty of a typical EELS experiment.

Tables 13−16 show the calculated geometries and vibrational frequencies for a number of H_3CO and H_2COH species. In all

TABLE 17: Calculated Properties of Methanol Cations, $[CH_3OH]^{+a}$

	method				
	MP2(full)/6-31G*	B3LYP/6-31G*	QCISD/6-31G*	MP2/6-311+G(2d,p)	MP2/6-311+G(2d,p)
$\langle s^2 \rangle$ before spin projection	0.7624	0.7539	NA	0.7668	0.7668
trans, R_{H-C}, Å	1.127	1.127	1.114	1.147	1.147
cis, R_{H-C}, Å	1.088	1.089	1.089	1.088	1.088
R_{O-C}, Å	1.382	1.369	1.404	1.352	1.352
R_{O-H}, Å	0.988	0.993	1.000	0.987	0.987
A_{HCO} (deg)	107.2	105.9	104.6	101.0	101.0
A_{HCO} (deg)	114.3	116.2	114.9	115.7	115.7
A_{COH} (deg)	114.2	114.3	114.0	113.8	113.8
frequency scaling factor	0.9427	0.9614	0.9537	unscaled	0.96
ν_1, cm^{-1}	217	257	15	226	217
ν_2, cm^{-1}	639	944	829	526	505
ν_3, cm^{-1}	961	953	972	958	919
ν_4, cm^{-1}	1005	1019	1007	1062	1019
ν_5, cm^{-1}	1214	1207	1222	1240	1190
ν_6, cm^{-1}	1276	1211	1276	1302	1250
ν_7, cm^{-1}	1315	1254	1286	1364	1309
ν_8, cm^{-1}	1444	1439	1436	1522	1461
ν_9, cm^{-1}	2601	2623	2777	2506	2405
ν_{10}, cm^{-1}	2933	2694	2788	3041	2919
ν_{11}, cm^{-1}	3083	3091	3096	3211	3083
ν_{12}, cm^{-1}	3300	3368	3313	3587	3444
electronic energy, hartree	−114.686419	−115.330886	−114.990091	−115.063892	

[a] We found two "stable" structures. This is data for the staggered structure (see text).

TABLE 18: Calculated Properties of Methanol Cations, $[CH_3OH]^{+a}$

	method	
	MP2/6-311+G(2d,p)	MP2/6-311+G(2d,p)
trans, R_{H-C}, Å	1.165	1.165
cis, R_{H-C}, Å	1.086	1.086
R_{O-C}, Å	1.296	1.296
R_{O-H}, Å	0.978	0.978
A_{HCO} (deg)	109.8	109.8
A_{HCO} (deg)	122.1	122.1
A_{COH} (deg)	113.7	113.7
frequency scaling factor	unscaled	0.96
ν_1, cm^{-1}	531	510
ν_2, cm^{-1}	919	882
ν_3, cm^{-1}	999	959
ν_4, cm^{-1}	1027	986
ν_5, cm^{-1}	1114	1069
ν_6, cm^{-1}	1327	1274
ν_7, cm^{-1}	1495	1435
ν_8, cm^{-1}	1742	1672
ν_9, cm^{-1}	2274	2183
ν_{10}, cm^{-1}	2672	2566
ν_{11}, cm^{-1}	3229	3100
ν_{12}, cm^{-1}	3695	3547
electronic energy, hartree	−115.066553	−115.066553

[a] We found two "stable" structures with MP2/6-311+G(2d,p). This is data for the eclipsed structure.

TABLE 19: Calculated Properties of Methoxonium Cations, $[CH_3OH_2]^+$

	method				
	MP2(full)/ 6-31G*	B3LYP/ 6-31G*	QCISD/ 6-31G*	MP2/6-311 +G(2d,p)	MP2/6-311 +G(2d,p)
R_{H-C}, Å	1.085	1.089	1.088	1.084	1.084
R_{O-C}, Å	1.516	1.522	1.522	1.513	1.513
R_{O-H}, Å	0.986	0.983	0.985	0.978	0.978
frequency scaling factor	0.9427	0.9614	0.9537	unscaled	0.96
ν_1, cm^{-1}	246	243	242	245	235
ν_2, cm^{-1}	730	700	746	749	719
ν_3, cm^{-1}	808	782	797	844	810
ν_4, cm^{-1}	907	905	914	952	914
ν_5, cm^{-1}	1131	1124	1134	1192	1145
ν_6, cm^{-1}	1244	1240	1250	1306	1254
ν_7, cm^{-1}	1427	1418	1426	1498	1438
ν_8, cm^{-1}	1446	1439	1445	1516	1455
ν_9, cm^{-1}	1447	1440	1446	1521	1460
ν_{10}, cm^{-1}	1633	1648	1663	1683	1616
ν_{11}, cm^{-1}	2990	3002	2993	3132	3006
ν_{12}, cm^{-1}	3126	3122	3118	3267	3137
ν_{13}, cm^{-1}	3135	3131	3127	3272	3141
ν_{14}, cm^{-1}	3378	3446	3435	3644	3499
ν_{15}, cm^{-1}	3465	3525	3515	3735	3585

cases the molecules are stable. There are some small differences among the vibrational frequencies at the various levels of calculation. However, all of the frequencies are the same within the uncertainty of a typical EELS experiment.

Tables 17 and 18 show vibrational frequencies for the triplet state of methanol cations. This case was different from all the rest in that the basis set had a significant effect on the results. According to the calculations, methoxy cations have two stable isomers: one with OH eclipsed with the methyl hydrogen, the second with the OH staggered. Only the staggered structure is stable at the MP2/6-31G*, B3LYP/6-31G*, and QCISD/6-31G* levels. However, both the eclipsed and staggered structures are stable at the MP2/6-311+G(2d,p) level. We have searched for a stable eclipsed structure at the B3LYP/6-311+G(2d,p) level but have not found one.

Table 19 shows the calculated geometries and vibrational frequencies for methoxonium ions. The geometries are almost all the same. There are some small differences among the vibrational frequencies at the various levels of calculation. The differences in frequency are within the uncertainty of a typical EELS experiment.

Finally, Table 20 shows the calculated geometries and vibrational frequencies for a hydrogen−hydroxymethyl cation complex. Here, there are some differences in the predicted geometries with changing method. However, all the frequencies are the same within the uncertainty of a typical EELS experiment.

Finally, Table 21 lists a few other species that we have considered. All are reasonable candidates, but all of these species decomposed or isomerized during the calculations.

Discussion

The results in Tables 1−20 show data for many species. We find that the calculated vibrational frequencies usually do not depend strongly on the method of calculation or the basis set used. There are few anomalous cases where B3LYP or QCISD fails. However, in the majority of examples we have considered, the results are largely independent of the calculational method or the basis set used.

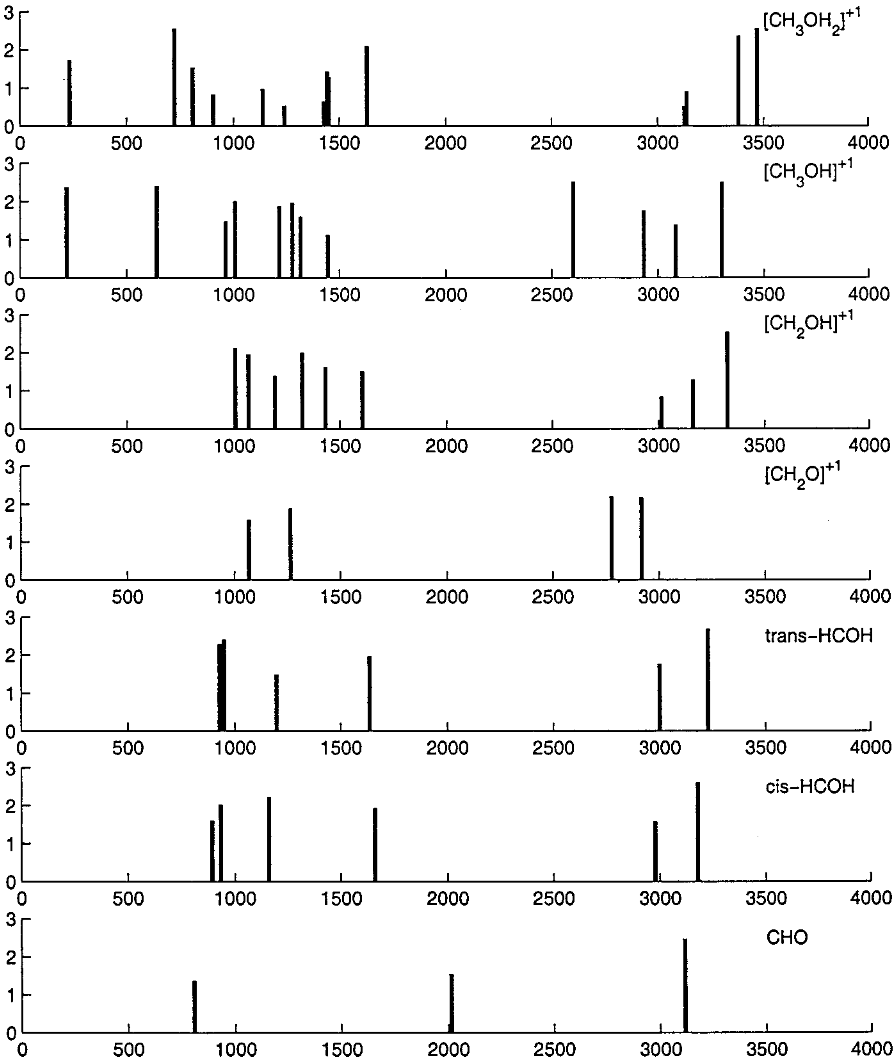

Figure 2. Charged (+1) species reference spectra calculated at the MP2(full)/6-31g* level. Plots are log(calculated intensity in arbitrary units) vs wavenumber (cm^{-1}).

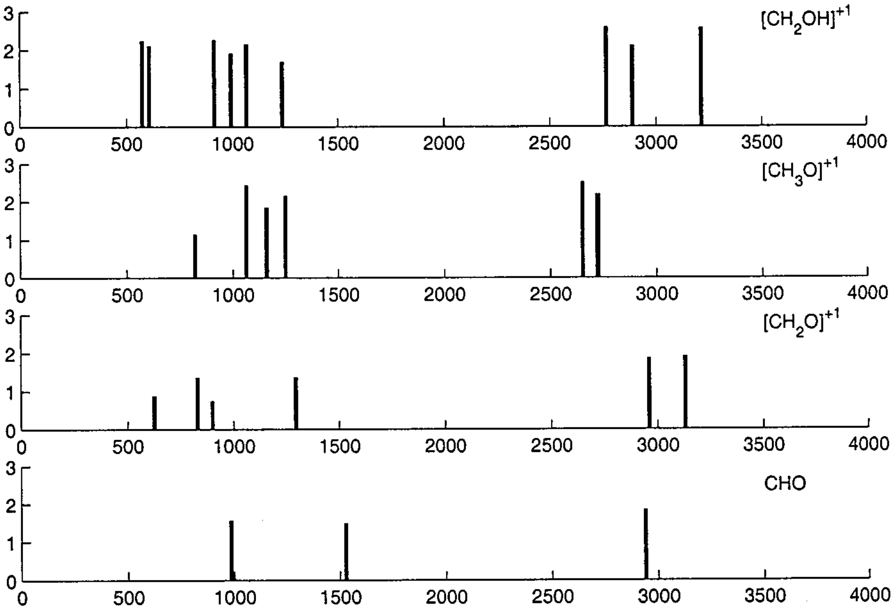

Figure 3. Excited-state charged (+1) species reference spectra calculated at the MP2(full)/6-31g* level. Plots are log(calculated intensity in arbitrary units) vs wavenumber (cm^{-1}).

Next, it is useful to compare all of our calculated reference spectra. Figure 1 shows the calculated spectra of all stable neutral species. Likewise, Figure 2 shows the spectra for the stable charged ground-state species and Figure 3 shows the

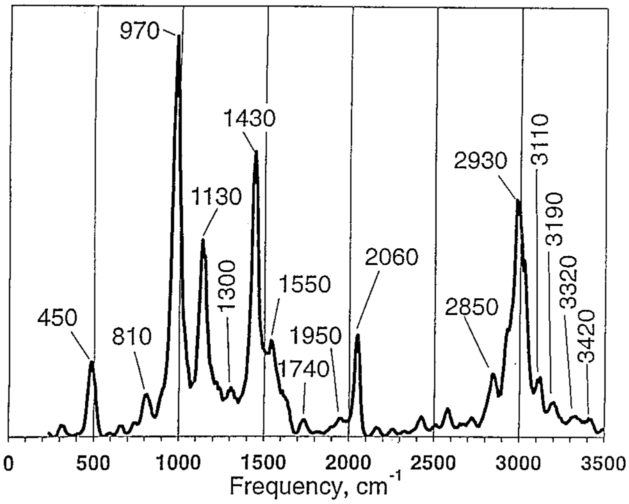

Figure 4. High-resolution HREELS of methanol and hydrogen coadsorbed on Pt(110). Scanning was done after dosing hydrogen at 273 K, cooling to 100 K, and dosing methanol.

stable excited species' spectra. While ab initio methods are not particularly good at predicting peak heights, the peaks in the figures here are the calculated heights.

We see that there are some trends in peak locations for the neutral species shown in Figure 1. The C−H stretches in the 3000 range shift to slightly lower frequencies for CHO and HCOH species. The OH stretches, though, shift only slightly down from about 3500 cm^{-1} as we move to the smaller molecules.

The C−O peak of CHO is very close to the 2000 cm^{-1} peak observed for carbon monoxide but is much lower in the other species. For the HCOH moieties, the C−O stretch is less than 1500 cm^{-1} and is only slightly lower for the larger species such as CH_2OH and CH_3OH. The CH_3 rock and umbrella motions are around 1000 cm^{-1} for both methanol and methoxy radical. Other COH bending frequencies in this same range appear in the smaller molecules, including the formyl radical.

Overall, we see that only formaldehyde and formyl radical have peaks between 1500 and 2500 cm^{-1}. However, only

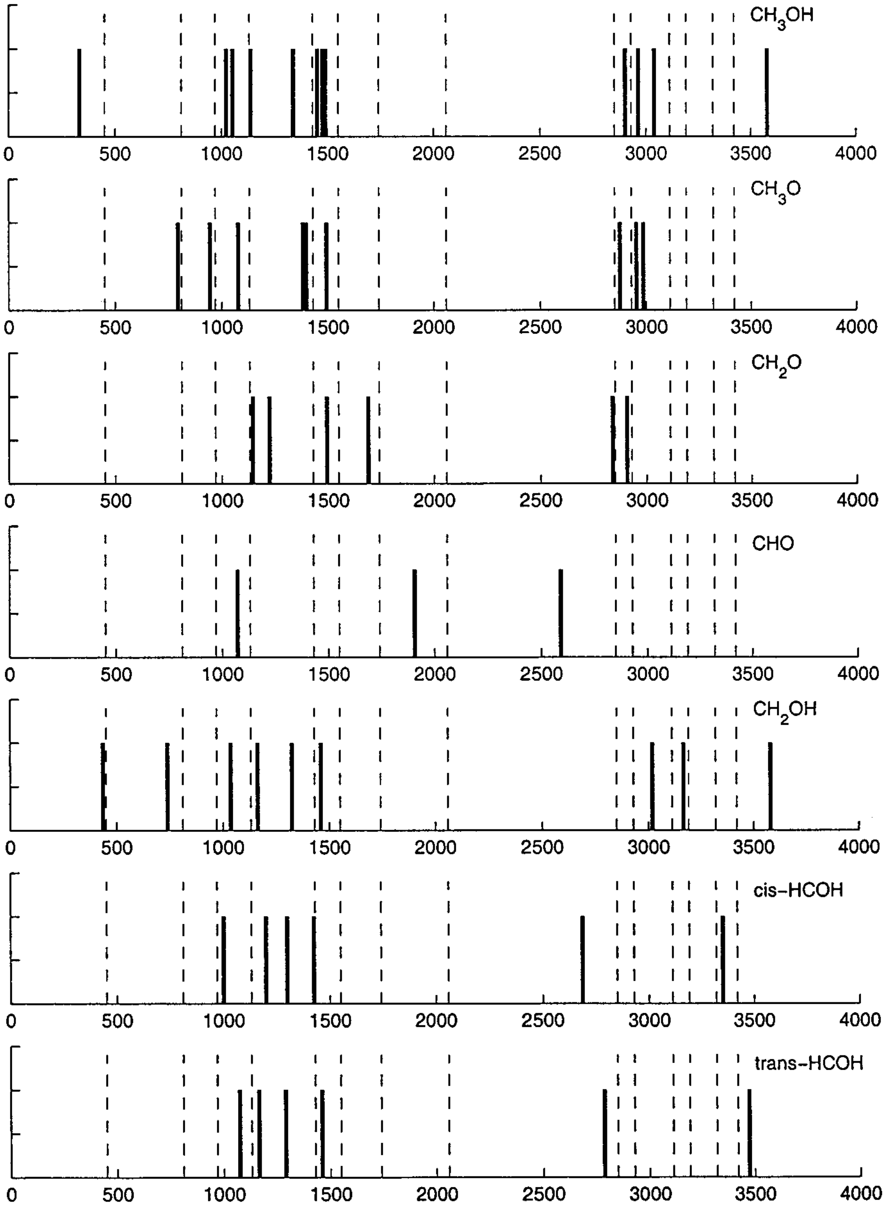

Figure 5. Neutral species reference spectra calculated at the MP2(full)/6-31g* level compared to experimental HREELS spectra of hydrogen and methanol coadsorbed on Pt(110). Plots are arbitrary intensity vs wavenumber (cm^{-1}) to allow comparison of peak locations.

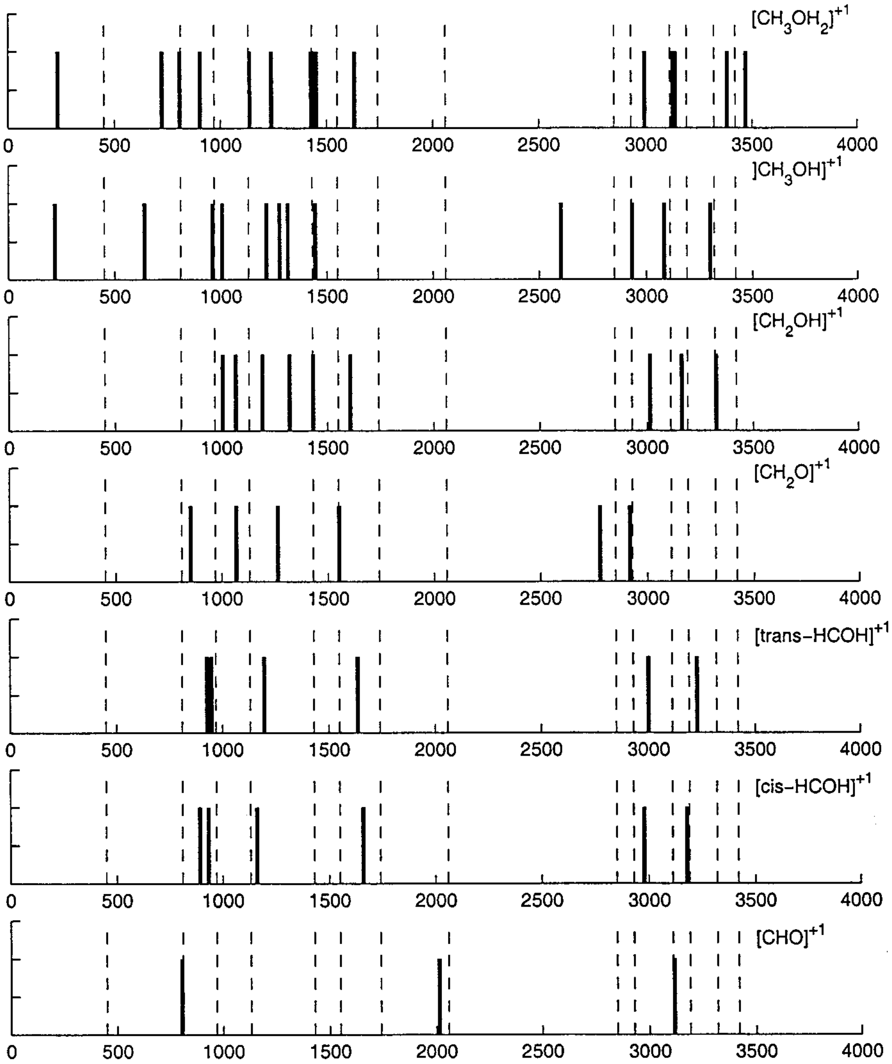

Figure 6. Charged (+1) species reference spectra calculated at the MP2(full)/6-31g* level compared to experimental HREELS spectra of hydrogen and methanol coadsorbed on Pt(110). Plots are arbitrary intensity vs wavenumber (cm^{-1}) to allow comparison of peak locations.

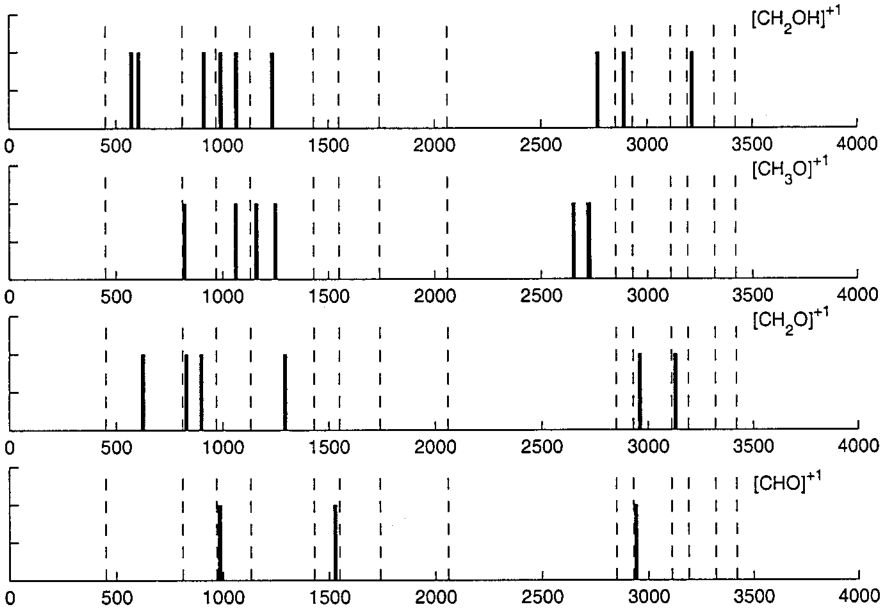

Figure 7. Excited-state charged (+1) species reference spectra calculated at the MP2(full)/6-31g* level compared to experimental HREELS spectra of hydrogen and methanol coadsorbed on Pt(110). Plots are arbitrary intensity vs wavenumber (cm^{-1}) to allow comparison of peak locations.

methanol and CH_2OH have peaks less than 500 cm^{-1}. Every species has peaks between 500 and 1500 cm^{-1}. Finally, methoxy, formaldehyde, and formyl radical all lack the higher O−H frequencies above 3000 cm^{-1}.

TABLE 20: Calculated Properties of a Stable $[CH_2O\cdots H]^+$ Planar Complex

	method				
	MP2(full)/ 6-31G*	B3LYP/ 6-31G*	QCISD/ 6-31G*	MP2/6-311 +G(2d,p)	MP2/6-311 +G(2d,p)
trans, R_{H-C}, Å	1.087	1.091	1.090	1.079	1.079
cis, R_{H-C}, Å	1.089	1.094	1.093	1.090	1.090
R_{O-C}, Å	1.256	1.250	1.259	1.248	1.248
R_{O-H}, Å	0.997	1.007	0.995	0.994	0.994
R_{H-H}, Å	2.017	1.701	3.038	1.789	1.789
A_{HCO} (deg)	121.8	122.0	121.8	121.4	121.4
A_{HCO} (deg)	122.8	122.2	122.7	122.7	122.7
A_{COH} (deg)	115.3	115.8	115.5	115.8	115.8
A_{OHH} (deg)	180	180	180	180	180
frequency scaling factor	0.9427	0.9614	0.9537	unscaled	0.96
ν_1, cm^{-1}	99	173	95	161	154
ν_2, cm^{-1}	161	249	156	248	238
ν_3, cm^{-1}	274	416	268	355	340
ν_4, cm^{-1}	1028	1030	1016	1107	1063
ν_5, cm^{-1}	1079	1094	1088	1152	1106
ν_6, cm^{-1}	1193	1187	1188	1249	1199
ν_7, cm^{-1}	1327	1336	1347	1413	1357
ν_8, cm^{-1}	1434	1430	1425	1509	1448
ν_9, cm^{-1}	1608	1621	1599	1686	1618
ν_{10}, cm^{-1}	3013	3002	3014	3131	3006
ν_{11}, cm^{-1}	3160	3043	3154	3283	3152
ν_{12}, cm^{-1}	3252	3141	3322	3403	3267

TABLE 21: Other Species That Were Examined[a]

species	charge	multiplicity	species	charge	multiplicity
cis-HCOH	1	4	CH_3OH_2	0	2
trans-HCOH	1	4	CH_3OH	1	4
CH_3O	1	1			

[a] All were unstable to isomerization.

The same kind of comparison can be done using the charged ground-state species. In Figure 2, we see that only methoxonium and methanol have peaks less than 500 cm^{-1}. Every stable species has peaks in the 2500−3500 cm^{-1} range. Only $[CHO]^{1+}$ does not have a peak between 1000 and 1500 cm^{-1}. Formyl is the only species, though, that has a peak near 2000 cm^{-1}.

In Figure 3 every charged excited species has at least one peak around 3000 and 1000 cm^{-1}. However, only $[CH_2O]^{1+}$ and $[CH_2OH]^{1+}$ have peaks around 600 cm^{-1}. On the basis of this figure, it would be difficult to distinguish among the charged excited-state species using IR spectroscopy.

To understand why these types of comparison are important, in previous work we saw a new species when hydrogen and methanol were coadsorbed on Pt(110).[40] The high-resolution EELS spectrum taken after dosing 0.5 L of hydrogen at 273 K and 3.0 L of methanol at 100 K is shown in Figure 4. There are peaks at 450, 810, 970, 1130, 1430, 1550, 1740, 1950, 2060, 2850, 2930, 3110, 3190, 3320, and 3420 cm^{-1}.

We established that the new species had one carbon atom, one oxygen atom, and an unknown number of hydrogen atoms. We strongly suspected the new species to be methoxonium $[CH_3OH_2]^+$, but a complete spectrum for methoxonium was not available in the literature. Reference spectra for other possible species were also lacking, particularly for the excited and charged states.

Figures 5−7 compare the calculated spectra to the spectrum of the new species that forms on Pt(110). These figures repeat Figures 2−4 with the calculated spectra represented with solid lines and the measured spectra represented with dashed lines. The differences in peak heights were ignored to make these figures.

Figure 5 compares the HREELS spectrum of the new species to the calculated spectra of all the neutral species considered in this paper. Note that the spectra of the neutral species do not match the new spectra well at all. In fact, combinations of various species do not even do that well. Methanol is missing most of the peaks in the 3000−3500 cm^{-1} region, as are all but the cis and trans forms of HCOH, which shows peaks around 3300−3450 cm^{-1}. Likewise, methanol is missing the 1740 cm^{-1} peak that appears only for formaldehyde. The only peak that does not appear in any of the calculated reference spectra is the 2060 cm^{-1} peak, which is a carbon monoxide peak.

Figure 6 shows a comparison of the experimental spectrum with the calculated reference spectra for the stable charged species. We see here that methoxonium agrees quite well with the observed spectrum. The peaks between 3000 and 3500 that were missing for methanol appear here. While there is no peak at 1740 cm^{-1}, the calculated spectrum is normally within ±60 cm^{-1}, which could place the 1631 peak much closer to the observed peak.

Figure 7 compares the HREELS spectrum to the calculated spectra for the excited charged states. We see that most of the 3000−3500 peaks are missing in these spectra for the excited charged states, as are most of the 1500−200 peaks.

So, using calculated reference spectra can allow surface scientists to rule out many possible species that do not have readily available complete experimental spectra. The formation of many neutral and charged species could be ruled out in this case because they do not show peaks in the right ranges compared to the measured EELS spectrum.

We also found that our calculations agreed very well with available spectroscopic and geometric information for the ground-state neutral species. The average absolute error in bond lengths was 0.06 Å, while angles were only incorrect by an average 0.3°. Also, our vibrational spectra peaks were within about 50 cm^{-1} of the experimental results.

Conclusions

In summary, we calculated the geometries and frequencies for the neutral, charged, and excited charged states of CH_3OH, CH_3O, CH_3OH_2, CH_2O, CH_2OH, CHO, and HCOH at several levels of calculation. We find good agreement with experimental geometries where they are available, with errors averaging 0.06 Å for bond lengths and 0.29° for angles. The average error in frequency calculations for the ground-state vibrational spectra was 48 cm^{-1} at the MP2/6-31g* level of calculation. Other results are presented that are largely in agreement with the MP2/6-31g* results. With these calculations, a consistent set of reference spectra is now available for a series of currently interesting molecules. This allows people in the surface science literature to use vibrational spectroscopy to examine a large class of molecules.

Acknowledgment. This work was funded by NSF Grant CTS 96-10115.

References and Notes

(1) R. I. Masel, *Principles of Adsorption and Reaction on Solid Surfaces*; Wiley and Sons: New York, 1996.

(2) Anderson, J. R. *Advances in Catalysis*; Academic Press: New York, 1973.

(3) Somorjai, G. *Introduction to Surface Chemistry and Catalysis*; Wiley: New York, 1981.

(4) Foster, J. J.; Masel, R. I. *Ind. Eng. Chem. Prod. Res. Dev.* **1986**, *25*, 563.

(5) Wang, J.; Masel, R. I. *J. Am. Chem. Soc.* **1991**, *113*, 5850.

(6) Seebauer, E. G.; Vohs, J. M.; Masel, R. I. *Ind. Eng. Chem. Fundam.* **1984**, *23*, 19.

(7) Wang, J.; Masel, R. I. *J. Vac. Sci. Technol. A* **1991**, *9*, 1879.

(8) Wang, J.; Masel, R. I. *Surf. Sci.* **1991**, *243*, 199.

(9) Olsen, C. W.; Masel, R. I. *Surf. Sci.* **1988**, *201*, 444.

(10) Olsen, C. W.; Masel, R. I. *J. Vac. Sci. Technol. A* **1988**, *6*, 792.

(11) Kyser, D. A.; Masel, R. I. *Rev. Sci. Instrum.* **1987**, *58*, 2141.

(12) Nigg, H. L.; Masel, R. I. *J. Vac. Sci. Technol. A* **1998**, *16*, 2581.

(13) Yagasaki, E.; Kishi, K. *J. Electron Spectrosc. Relat. Phenom.* **1994**, *69*, 133.

(14) Ohno, Y.; Matsushima, T.; Tanaka, S.; Yagasaki, E.; Kamada, M. *Surf. Sci.* **1992**, 281.

(15) Ma, N. L.; Smith, B. J.; Pople, J. A.; Radim, L. *J. Am. Chem. Soc.* **1991**, *113*, 7903.

(16) Bowman, J. M.; Bittman, J. S.; Harding, L. B. *J. Chem. Phys.* **1986**, *85*, 911.

(17) Bitterova, M.; Lischka, H.; Bishupic, S. *Int. J. Quantum Chem.* **1995**, *55*, 261.

(18) Iijima, T. *J. Mol. Struct.* **1989**, *212*, 137.

(19) Yanada, K.; Nakagawa, T.; Kuchitsu, K.; Morino, Y. *J. Mol. Spectrosc.* **1971**, *38*, 70.

(20) Nakagawa, T.; Morino, Y. *J. Mol. Spectrosc.* **1971**, *38*, 84.

(21) Bauschlicher, C. W.; Partridge, H. *Chem. Phys. Lett.* **1993**, *215*, 451.

(22) Gould, J. W.; Glukhovstsev, M. N.; Radom, L. *Chem. Phys. Lett.* **1996**, *262*, 187.

(23) Ma, N. L.; Smith, B. J.; Radom, L. *J. Phys. Chem.* **1992**, *96*, 5804.

(24) Glauser, W. A.; Koszykowski, M. L. *J. Phys. Chem.* **1991**, *95*, 10705.

(25) Martin, M. L.; Taylor, P. R.; Lee, T. J. *J. Chem. Phys.* **1993**, *99*, 286.

(26) Yates, B. F.; Yamaguchi, Y.; Schaeffer, H. F., III. *J. Chem. Phys.* **1990**, *93*, 8798.

(27) Gitino, E. L.; Pereira, A.; Ventura, O. N. *J. Chem. Phys.* **1995**, *102*, 2833.

(28) Frisch, M. J.; Trucks, G. W.; Head-Gorden, M.; Gill, P. M. W.; Wong, M. W.; Foresman, J. B.; Johnson, B. G.; Schlegel, H. B.; Robb, M. A.; Replogle, E. S.; Gomperts, R.; Andres, J. L.; Rahavachari, K.; Binkley, J. S.; Gonzalez, C.; Martin, R. L.; Fox, D. J.; Defrees, D. J.; Baker, J.; Stewart, J. J. P.; Pople, J. A. *Gaussian 92*, revision C; Gaussian, Inc.: Pittsburgh, PA, 1992.

(29) Frisch, M. J.; Trucks, G. W.; Schlegel, H. B.; Scuseria, G. E.; Robb, M. A.; Cheeseman, J. R.; Zakrzewski, V. G.; Montgomery, J. A., Jr.; Stratmann, R. E.; Burant, J. C.; Dapprich, S.; Millam, J. M.; Daniels, A. D.; Kudin, K. N.; Strain, M. C.; Farkas, O.; Tomasi, J.; Barone, V.; Cossi, M.; Cammi, R.; Mennucci, B.; Pomelli, C.; Adamo, C.; Clifford, S.; Ochterski, J.; Petersson, G. A.; Ayala, P. Y.; Cui, Q.; Morokuma, K.; Malick, D. K.; Rabuck, A. D.; Raghavachari, K.; Foresman, J. B.; Cioslowski, J.; Ortiz, J. V.; Stefanov, B. B.; Liu, G.; Liashenko, A.; Piskorz, P.; Komaromi, I.; Gomperts, R.; Martin, R. L.; Fox, D. J.; Keith, T.; Al-Laham, M. A.; Peng, C. Y.; Nanayakkara, A.; Gonzalez, C.; Challacombe, M.; Gill, P. M. W.; Johnson, B. G.; Chen, W.; Wong, M. W.; Andres, J. L.; Head-Gordon, M.; Replogle, E. S.; Pople, J. A. *Gaussian 98*, revision A.6; Gaussian, Inc.: Pittsburgh, PA, 1998.

(30) Pople, J. A.; Schlegel, H. B.; Krishnan, R.; DeFrees, D. J.; Binkley, J. S.; Frisch, M. J.; Whiteside, R. A.; Hout, R. F.; Hehre, W. J. *Int. J. Quantum. Chem. Symp.* **1981**, *15*, 269.

(31) Pople, J. A.; Anthony, P. S.; Wong, M. W.; Radom, L. *Isr. J. Chem.* **1981**, *33*, 345.

(32) Scott, A. P.; Radom, L. *J. Phys. Chem.* **1996**, *100*, 16502.

(33) Wong, M. W. *Chem. Phys. Lett.* **1996**, *256*, 391.

(34) Harmony, M. D.; Laurie, V. W.; Kuczkowski, R. L.; Schwendeman, R. H.; Ramsay, D. A.; Lovas, F. J.; Lafferty, W. J.; Maki, A. G. *J. Phys. Chem. Ref. Data* **1979**, *8*, 619.

(35) Osborn, D. L.; Leahy, D. J.; Newmark, D. M. *J. Phys. Chem. A* **1997**, *101*, 6583.

(36) Yamada, K.; Nakagama, T.; Kuchitsu, K.; Morino, Y. *J. Mol. Spectrosc.* **1971**, *38*, 70.

(37) Serrallach, A.; Meyer, R.; Gunthard, H. H. *J. Mol. Spectrosc.* **1979**, *52*, 94.

(38) Cui, Q.; Morkuma, K. *Chem. Phys. Lett.* **1996**, *263*, 54.

(39) Bouwens, R. J.; Hammerschmidt, J. A.; Grzeshowiak, M. M.; Stegnik, T. A.; Yorba, P. M.; Polk, W. F. *J. Chem. Phys.* **1996**, *104*, 460.

(40) Chen, N.; Blowers, P.; Masel, R. I. *Surf. Sci.* **1998**, *418*, 329.

(41) Sappey, A. D.; Crosley, D. R. *J. Chem. Phys.* **1990**, *3*, 7601.

(42) Tobiason, J. D.; Dunlop, J. R.; Rohlfing, E. A. *J. Chem. Phys.* **1995**, *103*, 1448.

(43) Hirota, E. *J. Mol. Struct.* **1986**, *146*, 237.

(44) Serrano-Andres, L. N.; Farsberg, P.; Malmqvist, P. Å. *J. Chem. Phys.* **1998**, *108*, 7202.

(45) Maurue, D.; Head-Gordon, M. *Mol. Phys.* **1999**, *96*, 1533.